

6th CIRP Conference on Surface Integrity

# Main time-parallel mechanical surface treatment and surface texturing during machining

Jannik Schwalm<sup>a,\*</sup>, Felix Mann<sup>b</sup>, Michael Gerstenmeyer<sup>a</sup>, Frederik Zanger<sup>a</sup>, Volker Schulze<sup>a</sup>

<sup>a</sup>*wbk Institute of Production Science, Karlsruhe Institute of Technology (KIT), Kaiserstr. 12, 76131 Karlsruhe, Germany*

<sup>b</sup>*Faculty of Mechanical Engineering, Karlsruhe Institute of Technology (KIT), Kaiserstr. 12, 76131 Karlsruhe, Germany*

\* Corresponding author. Tel.: +49-721-608-42455; fax: +49-721-608-45004. E-mail address: [jannik.schwalm@kit.edu](mailto:jannik.schwalm@kit.edu)

## Abstract

The microtexture of surfaces in tribological contact influences the tribosystem and can be adjusted by the process parameters during turning. However, the limited dynamics of the machine tool restrict this and usually only allow adjustment by kinematic roughness. In this work, a novel combined process for surface texturing by plastic deformation of the surface layer, using a piezoelectric tool system that enables highly dynamic positioning of cutting tools, is presented. During turning, process forces are measured and confocal microscopy images are used to analyse the topography. The investigations are analysed in more detail with the help of kinematics simulations.

© 2022 The Authors. Published by Elsevier B.V.

This is an open access article under the CC BY-NC-ND license (<https://creativecommons.org/licenses/by-nc-nd/4.0>)

Peer review under the responsibility of the scientific committee of the 6th CIRP CSI 2022

*Keywords:* surface texturing; mechanical surface treatment; piezoelectric tool system

## 1. Introduction

More and more complex process chains demand innovations in manufacturing strategies for the production of high-performance components. The focus here is on the surface layer of such components, as it has a crucial influence on their behaviour, such as fatigue strength and wear resistance. This can be specifically adjusted by mechanical surface treatment processes. Surface treatments can be divided into unguided processes such as shot peening or with a guided tool. The last can be subdivided into burnishing, without an additional movement component normal to the surface, and machine hammer peening (MHP) [1]. The latter is a vibration-superimposed process. Piezoelectric systems represent a possible type of actuation in this case. These processes can be divided into resonant systems, which work with a sonotrode, and strictly piezoelectric systems [2]. These systems allow a mechanical surface treatment and a modification of the surface layer. The mechanisms of hardening here are based on an

elastic-plastic deformation of the surface layer [3]. This permanent deformation results in a change of the topography [4], which enables optimisation for tribological applications [5-7]. Microtexturing of the surface can be achieved by vibration-assisted tools. The use of such highly dynamic tools for controlled texturing during machining has been implemented on conventional lathes up to a frequency of 135 Hz [8]. The tool is moved in one spatial direction. A reduction of the friction coefficient could be shown by such a textured surface [9]. However, the microtexture is formed during machining, where the plastic deformation of the surface layer is minimal and no dominant hardening occurs. In this paper, the innovative combined process hammering turning is presented that allows microtexturing by plastic deformation of the surface layer with the tool during machining. The process forces, the topography and the complex dynamic behaviour of the tool system were investigated, both experimentally and by means of kinematics simulation.

Nomenclature	
$A_{c,o}$	Amplitude cutting direction
$A_h$	Stroke hammering
$d_i$	Distance of the indentations (cutting direction)
$f_c$	Axial feed
$f_{c,o}$	Main frequency (cutting direction)
$f_h$	Frequency oscillation (hammer direction)
$r_\beta$	cutting edge rounding
$r_e$	Nose radius
$S_p$	Maximum peak height
$S_v$	Maximum sink height
$S_z$	Maximum height
$t_h$	Time of the hammer stroke
$v_c$	Cutting velocity
$v_{c,eff}$	Effective cutting velocity
$v_{c,o}$	Velocity of oscillation (derivative of deflection)
$\alpha$	clearance angle
$\gamma$	rake angle

### 1.1. Process description hammering turning

The intention of hammering turning is to combine mechanical surface treatment and surface microtexturing during machining simultaneously. This means integrating the conventionally subsequent step of mechanical surface treatment and microtexturing into the machining process at the same time. In this innovative combined process, the mechanical surface treatment is to be carried out by the cutting tool. A hammering movement of the tool causes a plastic deformation of the surface layer. To enable the hammering movement of the tool, it is necessary to decouple this movement from machining. For this purpose, the tool is oscillated with the help of a piezo actuator. The amplitude of this oscillation is superimposed to the cutting process. Since the tool has a periodical movement direction with and against the cutting direction due to the oscillation, the superimposition with the cutting velocity results in minima of the relative velocity between tool and workpiece. In these minima, the tool performs a hammering movement normal to the workpiece surface. This hammering stroke has a time period of 1/3 of the superimposed oscillation in the cutting direction. The bidirectional superimposed movement of the tool is shown schematically in Figure 1. The hammering stroke of the tool is similarly caused by a piezo actuator. In this piezoelectric tool

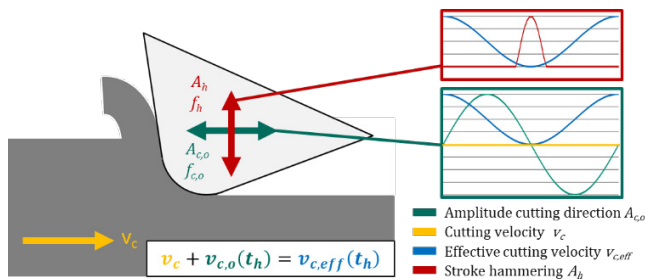


Figure 1: Schematic visualisation of hammering turning

system, the displacement is not achieved by resonant oscillation, as in many vibration-assisted machining (VAM) systems [10,11], but rather by forced oscillation. The description of the movement in the cutting direction of the tool system as a harmonic oscillation is not correct from a physical point of view, since the displacement is not caused by the inertia of a mass and a returning force proportional to the displacement. It is a highly dynamic periodic positioning of the tool system in accordance with a harmonic oscillation. This allows maximum flexibility of the process parameters for hammering turning, as amplitude, frequency and oscillation mode can be set freely and independently of each other. In this way, complex modes of oscillation can also be investigated that cannot be represented by a harmonic oscillation.

### 1.2. Kinematic constraint

The temporary decoupling of cutting and hammering requires a constraint on the movement. In order to achieve the highest possible amount of plastic deformation of the surface, this must be decoupled from the cutting and take place at a minimum of the effective velocity between the workpiece and the tool. The kinematic constraint for hammering turning is defined by

$$v_c + v_{c,o}(t_h) = v_{c,eff}(t_h) \quad (1)$$

$$v_{c,eff}(t_h) = 0 \quad (2)$$

$$-v_c = v_{c,o}(t_h)$$

With a sinusoidal oscillation in the direction of cutting, the displacement  $x_o$  and the derived velocity  $\dot{x}_o$  result in

$$x_o(t) = \sin(2\pi * f_{c,o} * t) * A_{c,o} \quad (3)$$

$$\dot{x}_o(t) = v_{c,o}(t) = \cos(2\pi * f_{c,o} * t) * (2\pi * f_{c,o}) * A_{c,o} \quad (4)$$

$$-v_c = \cos(2\pi * f_{c,o} * t) * (2\pi * f_{c,o}) * A_{c,o}$$

From this, the relationship between amplitude  $A_{c,o}$ , frequency  $f_{c,o}$  and cutting velocity  $v_c$  of a harmonic sinusoidal oscillation for a maximum cutting velocity results in

$$\min[-v_c] = \min[\cos(2\pi * f_{c,o} * t)] * (2\pi * f_{c,o}) * A_{c,o} \quad (5)$$

$$\min[-v_c] = -1 * (2\pi * f_{c,o}) * A_{c,o}$$

$$\max[v_{c,eff}] = 2 * v_c$$

$$\min[v_{c,eff}] = 0$$

The distance between the tool indentations  $d_i$  and the kinematic constraint of the process parameters is given by

$$f_{c,o} = \frac{v_c}{2\pi * A_{c,o}} \quad (6)$$

$$d_i = v_c * \frac{1}{f_{c,o}} = 2\pi * A_{c,o} \quad (7)$$

The correlation of the amplitude and cutting velocity on the corresponding frequency can be clearly seen. By selecting other modes of oscillation, such as an asymmetrical triangular signal oscillation, it is possible to increase the cutting velocity and the distance between the indentations for given conditions.

## 2. Setup

### 2.1. Simulation setup

For the prediction of the microtexture, a kinematics simulation was implemented in the MATLAB development environment to analyse the influence of the process parameters axial feed  $f_c$ , hammer stroke  $A_h$  and tool microgeometry. An area of  $550 \mu\text{m} \times 550 \mu\text{m}$  was calculated with a discretisation  $< 1 \mu\text{m}$ . The tool microgeometry is first discretised as a stl-file. From this discretised tool, a single indentation is calculated, which is subtracted multiple times from a surface according to the specified process parameters. The kinematic roughness is calculated as a function of the tool nose radius  $r_e$  and the axial feed  $f_c$ . This provides the ideal microtexture after the hammering turning. Compared to an FEM simulation, this simulation enables an effective calculation with a very precise discretisation. A disadvantage of this simulation method is that no physical material behaviour can be represented, which is why it is not suitable for the simulation of process forces. However, this simulation method makes it possible to determine the idealised topography with very short computing time and very high resolution, from which it is possible to calculate the height parameters according to ISO 25178. Based on the height parameters  $S_v$ ,  $S_p$  and  $S_z$ , a validation with the measured microtexture was possible. Figure 2 shows an example of the simulated microtexture (Figure 2 a) compared to the measured microtexture (Figure 2 b).

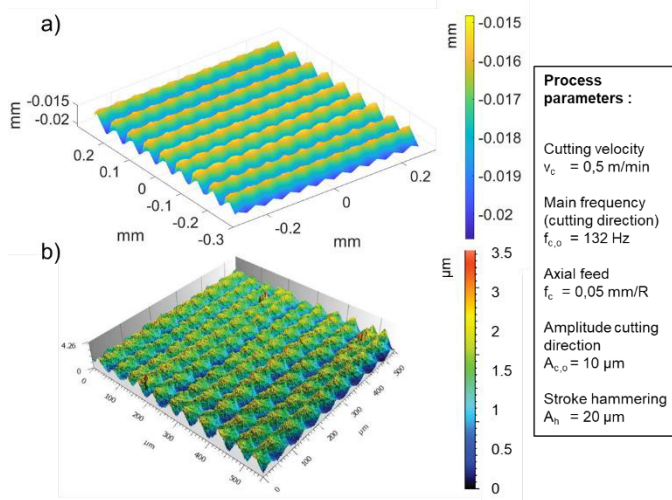


Figure 2: Simulated topography a) and measured topography b)

### 2.2. Experimental Setup

In this work, experimental evidence of the suitability and controllability of hammering turning is provided. In the experiments, the combined process hammering turning, as well as its partial processes external longitudinal turning, external longitudinal turning with superimposed oscillation in the cutting direction and external longitudinal turning with superimposed hammering perpendicular to the surface, was investigated. This enables a separate evaluation of the process forces of the partial processes. Mechanical surface treatment and microtexturing were carried out using standard cutting inserts (uncoated cermet material NX2525, type CCMW

120404), which have a nose radius of  $r_e = 0.4 \text{ mm}$  and a cutting edge rounding of  $r_\beta = 30 \mu\text{m}$ . In the experiments, shafts made of quenched and tempered 42CrMo4 (AISI 4041,  $R_e = 970 \text{ MPa}$ ,  $R_m = 1080 \text{ MPa}$ ) were processed by hammering turning, based on external longitudinal turning. The axial feed  $f_c$  and the cutting velocity  $v_c$ , limited by the maximum frequencies of the piezo actuators, were varied during the experiments. Due to the kinematic coupling, there is a correlation between cutting velocity  $v_c$  and main frequency  $f_{c,o}$  (see chapter 1.2). The process parameters can be found in Table 1. In the investigations a rake angle of  $\gamma = 0^\circ$  and a clearance angle  $\alpha = 7^\circ$  were used. The experiments were set up on a vertical CNC turning centre of the type Vertical Line V100 from Index-Werke. The parallel kinematics of this type of lathe has a high rigidity and enables the stationary installation of the piezoelectric tool system. The process forces were measured using a force measurement platform (9257B) and charge amplifiers (5015A) from Kistler Instrumente. Data acquisition was carried out with a measuring card (DT 322) from the manufacturer DATA Translation and the software MATLAB and data evaluation was done in the software OriginPro. The measurement signals were sampled at a frequency of 75 kHz. At this high sampling frequency, it was ensured that the Nyquist-Shannon sampling theorem was also fulfilled for higher-frequency oscillations and that frequencies up to at least 35 kHz could be evaluated. The topography was measured and evaluated optically using a confocal light microscope from Nanofocus and the analysis software  $\mu\text{soft}$  analysis. This enables a three-dimensional evaluation of the textured surfaces. The determination of the height parameters was carried out according to ISO 25178 on an area with the same size as in the simulations of  $550 \mu\text{m} \times 550 \mu\text{m}$ .

Table 1: Process parameters for hammering turning

Process parameters	Value
Cutting velocity $v_c$ [m/min]	0.5, 1, 2, 3.5
Related main frequency $f_{c,o}$ [Hz]	133, 265, 531, 928
Axial feed $f_c$ [mm/rev]	0.05, 0.1, 0.2
Cutting depth $a_p$ [mm]	0.1
Amplitude oscillation $A_{c,o}$ [ $\mu\text{m}$ ] (sinusoidal)	10
Stroke hammering $A_h$ [ $\mu\text{m}$ ]	20

### 2.3. Design of the piezoelectric tool system

The tool system is designed as a highly dynamic piezoelectric system. This system can be displaced up to  $20 \mu\text{m}$  by two perpendicularly arranged piezo actuators. The deflection of the actuators deforms a biaxial solid flexure hinges made of aluminium. This is designed in a dual parallel kinematic arrangement in order to keep the tilting of the tool as low as possible. The actuators are located in a plane perpendicular to the surface of the workpiece and tangentially in the cutting direction. Since the actuators are not able to receive larger tensile forces, but only compressive forces, an active repositioning of the tool system is necessary. Active repositioning is ensured by a spring preload of 300 N. The springs are equipped with damping elastomer elements to

prevent natural oscillations. The design of the tool system is demonstrated in Figure 3. The piezo actuators are custom-made and are controlled with a voltage of  $\pm 30$  V. They have a maximum compressive load of 3000 N at a stiffness of 100 N/ $\mu\text{m}$ . The piezo amplifiers are a continuous amplifier and a pulser, both of which are also special electronics with maximum currents of up to 20 A and a maximum frequency of up to 3000 Hz. The piezo amplifiers are controlled by a 2 channel arbitrary function generator (MFG-2230M) from the manufacturer GW Instek.

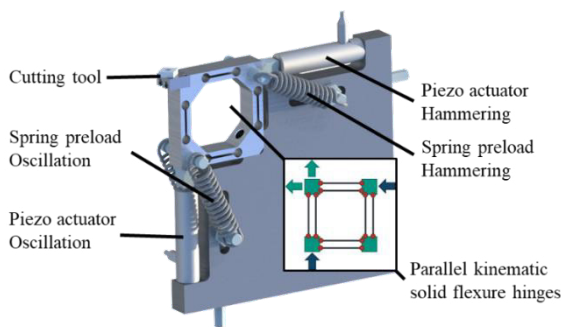


Figure 3: Design of the piezoelectric tool system for hammering turning

### 3. Results and discussion

Figures 4 - 7 compare the process forces for hammering turning and the partial processes for the cutting velocity and feed rates investigated. The X direction represents the direction of the hammering and the passive force, the Y direction represents the cutting force and Z is the axial feed force. For each parameter set the mean values of the forces are of a similar order of magnitude for the 3 partial processes as well as for the hammering turning. This is to be expected because the forces also oscillate due to the oscillation of the tool, but they must be similar in their average. Mathematically, the superimposed oscillation in the cutting direction leads to an effective cutting velocity between  $v_{c,eff} = 0$  and  $v_{c,eff} = 2 v_c$ , but the mean value of the cutting velocity is  $v_c$ . Figure 4 presents the process forces for a main frequency of  $f_{c,o} = 133$  Hz resp.  $v_c = 0.5$  m/min.

Comparing the turning and the oscillation superimposed turning at a feed rate of  $f_c = 0.2$  mm/rev, a small decrease in the average forces can be observed. The maximum cutting force is also slightly lower. The oscillation of the tool in the cutting direction leads only to a small increase of the difference between min and max force. This is surprising in the case of oscillation superimposed turning, since due to the calculated difference of the effective cutting velocity, its force should also have a larger difference. Since there is also an elastic deformation of the tool holder in the process, it is to be expected that the minimum of the cutting forces does not go towards zero, but remains at a higher level. From this it can be assumed that the oscillation in the cutting direction does not have a dominant influence. Considering the partial process of hammer superimposed turning, this leads to a completely different characteristic of the process forces. The hammering of the tool can also be clearly observed in the passive forces as a significant difference between maximum and minimum force. The minimum force even becomes native here. Since there is no superimposed oscillation in the cutting direction to decouple and remove the load from the tool, negative forces can occur on the tool when it is retracted after hammering. But not just this can result in negative forces, the mass inertia of the tool and the tool holder must also be considered. This is most pronounced at a small feed of  $f_c = 0.05$  mm/rev. The influence of hammering on the other two force components is also visible. Here the difference between minimum and maximum force also increases significantly. Due to the hammering of the tool perpendicular to the surface, this also causes an oscillating cutting depth, while the cutting velocity remains constant. The increased difference of the cutting force can result from this. The same applies to the feed force, due to the cyclic indentation of the tool. Since there is considerably more material on one flank of the nose radius, there is a lateral cyclic force component that leads to a noticeable difference. When considering the hammering turning, which is a combination of the three partial processes, it is obvious that the forces must also be a combination of these. Since no cutting should be carried out here during the hammering, this also reduces the forces of the hammering marginally. The process at a main

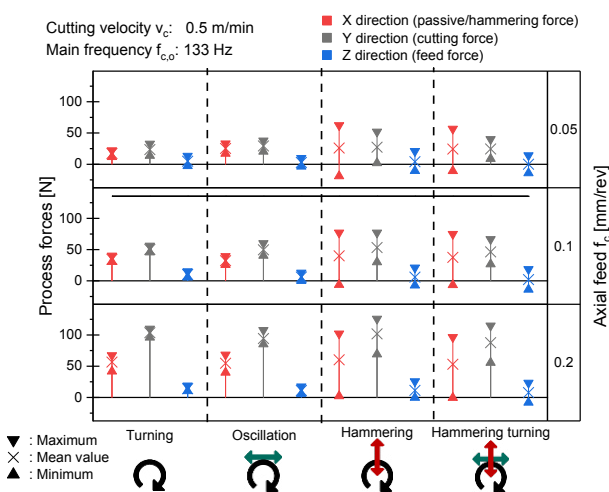


Figure 4: Process forces in hammering turning and the partial processes at a main frequency  $f_{c,o} = 133$  Hz, cutting velocity  $v_c = 0.5$  m/min

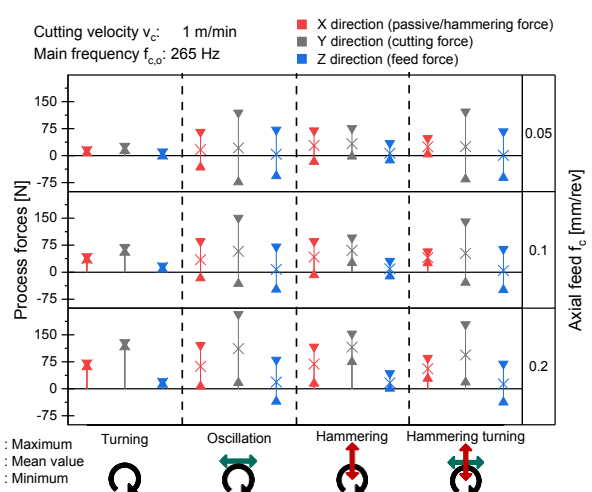


Figure 5: Process forces in hammering turning and the partial processes at a main frequency  $f_{c,o} = 265$  Hz, cutting velocity  $v_c = 1$  m/min

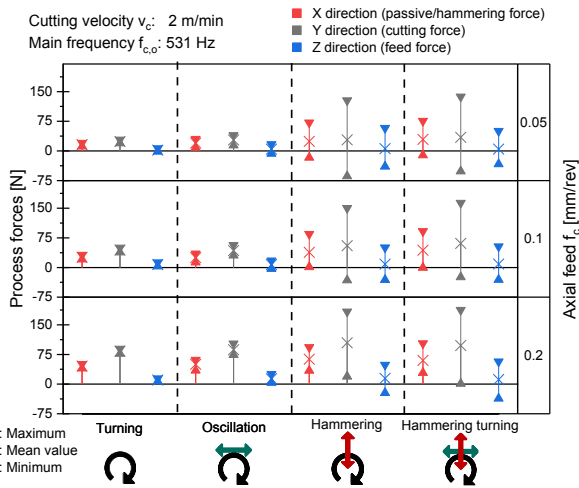


Figure 6: Process forces in hammering turning and the partial processes at a main frequency  $f_{c,0} = 531$  Hz, cutting velocity  $v_c = 2$  m/min

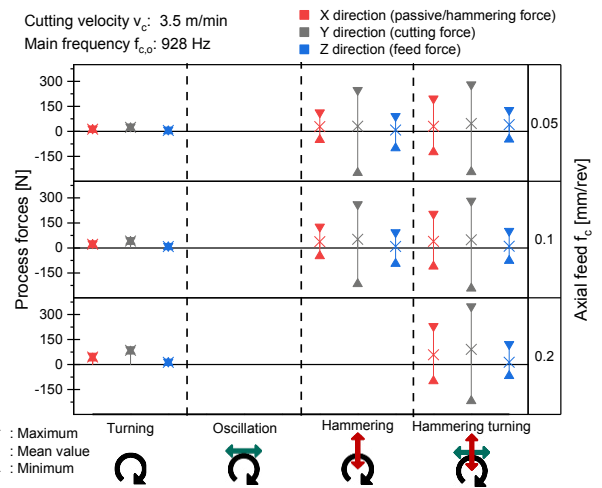


Figure 8: Process forces in hammering turning and the partial processes at a main frequency  $f_{c,0} = 928$  Hz, cutting velocity  $v_c = 3.5$  m/min

frequency of  $f_{c,0} = 133$  Hz seems to be clearly characterised by the hammering partial process. Figure 5 presents the process forces for the partial processes as well as the hammering turning at a main frequency of  $f_{c,0} = 265$  Hz resp.  $v_c = 1$  m/min. It can be observed that for turning, the mean value as well as the minimum and maximum value for all force components are close together. In contrast to the process forces for  $f_{c,0} = 133$  Hz, a significant difference of the forces can be seen in the case of oscillation superimposed turning. This is to be expected due to the oscillating cutting velocity. The process forces become negative at a small feed  $f_c = 0.05$  mm/rev, which is not consistent with the process mechanism, where separation is not intended. The magnitude of the difference between minimum and maximum forces is hardly influenced by the axial feed. Since the mean value is in good agreement with the turning, this suggests that this is due to dynamic inertia effects of the tool system. In the case of hammer superimposed turning, the difference of the process forces is also similarly unaffected, only the mean value changes with the feed. In this case, the hammering turning has the characteristics of the partial process of oscillation superimposed turning and is dominated by it. The mean values of the hammering forces are reduced in hammering turning compared to hammering superimposed turning, which is not to be expected. The reason for this could be the separation detected during oscillation. Figure 6 shows the process forces for the partial processes as well as the hammering turning at a main frequency of  $f_{c,0} = 531$  Hz resp.  $v_c = 2$  m/min. The same characteristics of the process can be seen here as at  $f_{c,0} = 133$  Hz, which is dominated by the partial process of hammering superimposed turning. Therefore, the dominant force component is the cutting force. At a low feed rate of  $f_c = 0.05$  mm/rev the minimum cutting force is even significantly negative. This suggests that the hammering causes a strong oscillation in the orthogonal cutting direction. Figure 8 shows the process forces for the partial processes as well as the hammering turning at a main frequency of  $f_{c,0} = 928$  Hz resp.  $v_c = 3.5$  m/min. Due to measurement failures, the results for the partial process of oscillation superimposed turning are missing here. The largest difference of the cutting forces can be seen in the partial

processes hammering superimposed turning and hammering turning. This indicates that the process is dominated by hammering superimposed turning, like the process at  $f_{c,0} = 133$  Hz and 531 Hz. It can be observed that there is a very large difference of the process forces, and the process is strongly influenced by these peak forces. Since the different dominance of the partial processes is hardly influenced by the feed rate  $f_c$ , this shows that the process exhibits highly dynamic behaviour. These results show that the hammering turning process cannot be equated with a steady-state external longitudinal turning process. The excitation of the tool in two axes leads to an especially complex dynamic behaviour, which causes a complex system response. Figure 7 shows the measured and simulated height parameters  $S_p$  (maximum peak height),  $S_v$  (maximum valley height) and  $S_z$  (maximum height). These values are given as a function of the axial feed  $f_c$  and the cutting velocity  $v_c$  respectively the main frequency  $f_{c,0}$ . Since the kinematic simulation is a merely geometric model, the cutting velocity has no influence on the result, only the axial

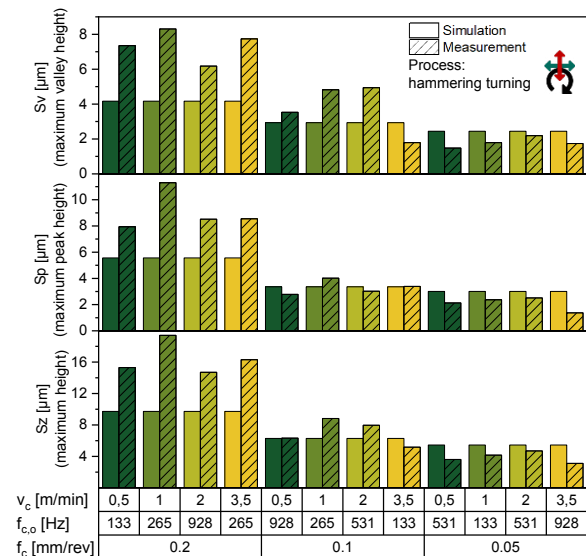


Figure 7: Measured and simulated height parameters  $S_p$ ,  $S_v$  and  $S_z$  of the topography after hammering turning.

feed  $f_c$ . Therefore, the same value is always present for the simulation within a group. In the experimental investigation, the influence of the cutting velocity is obviously present. On the one hand, in addition to kinematic roughness, there is a process-related roughness caused by the cutting process and irregularities. On the other hand, a complex oscillating system is present in the experiment, which responds to different excitation with different amplitudes and modes. Although the system should not oscillate resonantly, this excitation cannot be avoided in the real system. It can be seen that the differences between simulated and measured topography are greatest at a feed of  $f_c = 0.2$  mm. It can be assumed that the formation of the kinematic roughness during turning has a greater influence. This is represented in the simulation, but only geometrically. Plastic deformations caused by the hammering, which are also added to the peak crests, cannot be represented. Nevertheless, there is a good correlation between the simulation and the experimentally determined value. At a feed rate of  $f_c = 0.1$  mm/rev the simulation predicts too low values of  $S_v$  (maximum valley height), as well. Since the simulation does not show any material throw up, it is possible that additional throw ups increase the maximum valley height by the indentation. The discrepancy can also be caused by process irregularities. In the confocal microscope images, there were singular grooves in the topography, which were probably caused by adhesions on the cutting edge. These grooves are deeper than the textured surface and can increase the values. At the smallest feed rate investigated ( $f_c = 0.05$  mm/rev) the simulated values are slightly higher. One possible reason for this is the elastic springback of the material in this small size dimension. Also, the small axial distance between the tool paths can lead to a partial replacement of the indentations by the material flow during a further tool pass. It is especially significant that the simulated value of the  $S_z$  (maximum height) does not exceed  $9.7 \mu\text{m}$ , although the stroke of the hammering is larger and material throw up is still to be expected. Since this is the ideal topography, this effect is based on the process parameters. The overlapping of the tool indentations leads to a maximum height smaller than the stroke of the hammer movement. It can be shown that this merely geometric simulation is able to approximate the topography after hammering turning. Therefore, it is possible to make estimations of the resulting topography and microtexture with this geometric simulation.

#### 4. Conclusion and outlook

In this paper, the novel combined process of hammer turning was presented, which includes mechanical surface microtexturing with the cutting tool during machining. For this purpose, the tool is oscillated biaxially, which results in a periodic microtexturing caused by plastic deformation due to strokes perpendicular to the surface with the tool. In the study, a geometric simulation was presented to predict the microtexture, which was validated using the height parameters  $S_v$ ,  $S_p$  and  $S_z$ . The best correlation was observed for an axial feed of  $f_c = 0.1$  mm/rev. A consideration of the process forces of the partial processes and those of the hammering turning

showed different dynamic characteristics of the system depending on the main frequency respectively the cutting velocity. At frequencies of 133 Hz, 531 Hz and 928 Hz, the hammering superimposed on the turning is the dominant process force. At a frequency of 265 Hz the oscillation superimposed on the turning process is dominant for the hammering turning. In order to further analyze the complex dynamic characteristics of the system, the piezoelectric tool system is to be supplied with a contactless inductive position measuring system. This enables a correlation of the process forces with the excitation signals. In this way, the actual displacements can be determined, as well as a phase shift between the input signal and the displacement. This allows the experimental evidence to prove that the surface texture is caused by plastic deformation and not by cutting. Furthermore, the tribological properties of the microtexture will be investigated.

#### Acknowledgements

The authors thank the German Research Foundation for funding this study as part of the research project ZA 785/4-1.

#### References

- [1] Schulze, V., Bleicher, F., Groche, P., Guo, Y.B., Pyun, Y.S., 2016. Surface modification by machine hammer peening and burnishing. *CIRP Annals* 65 (2), 809–832.
- [2] Chan, W.L., Cheng, H.K.F., 2021. Hammer peening technology—the past, present, and future. *Int J Adv Manuf Technol* 718 (110), 10.
- [3] Bleicher, F., Lechner, C., Habersohn, C., Kozeschnik, E., Adjassoho, B., Kaminski, H., 2012. Mechanism of surface modification using machine hammer peening technology. *CIRP Annals* 61 (1), 375–378.
- [4] Steitz, M., Scheil, J., Müller, C., Groche, P., 2013. Effect of Process Parameters on Surface Roughness in Hammer Peening and Deep Rolling. *KEM* 554-557, 1887–1901.
- [5] Klocke, F., Trauth, D., Schongen, F., Shirobokov, A., 2014. Analysis of friction between stainless steel sheets and machine hammer peened structured tool surfaces: experimental and numerical investigation of the lubricated interaction gap. *Prod. Eng. Res. Dev.* 8 (3), 263–272.
- [6] Pyoun, Y.S., Park, J.H., Suh, C.M., Amanov, A., Kim, J.H., 2011. Friction and Wear Characteristics of SUS304 and SUS630 after Ultrasonic Nanocrystal Surface Modification. *AMR* 275, 174–177.
- [7] Steitz, M., Stein, P., Groche, P., 2015. Influence of Hammer-Peened Surface Textures on Friction Behavior. *Tribol Lett* 58 (2), 404.
- [8] Kurniawan, R., Ko, T.J., 2013. A study of surface texturing using piezoelectric tool holder actuator on conventional CNC turning. *Int. J. Precis. Eng. Manuf.* 14 (2), 199–206.
- [9] Kurniawan, R., Ko, T.J., 2015. Friction reduction on cylindrical surfaces by texturing with a piezoelectric actuated tool holder. *Int. J. Precis. Eng. Manuf.* 16 (5), 861–868.
- [10] Brehl, D.E., Dow, T.A., 2008. Review of vibration-assisted machining. *Precision Engineering* 32 (3), 153–172.
- [11] Greco, A., Raphaelson, S., Ehmann, K., Wang, Q.J., Lin, C., 2009. Surface Texturing of Tribological Interfaces Using the Vibromechanical Texturing Method. *Precision Engineering* 131 (6), 430.